Journal of Radioanalytical and Nuclear Chemistry (2024) 333:2557–2565
https://doi.org/10.1007/s10967-023-09033-w

# Environmental radioactivity measurements in soil using inductively coupled plasma mass spectrometry and gamma-ray spectrometry in various areas in Cameroon

**Modibo Oumar Bobbo[1,2] · Guosheng Yang[3] · Saïdou[1,2] · Hirofumi Tazoe[4] · Naofumi Akata[4] · Chutima Kranrod[4] · Masahiro Hosoda[4] · Shinji Tokonami[4]**

Received: 17 January 2023 / Accepted: 28 June 2023 / Published online: 13 July 2023


**Abstract**
In this study, data from the first measurement of $^{236}$U in surface soil samples in Cameroon are reported, with the primary objective of establishing baseline data in the case of the accidental release of nuclear fuel to the environment in the future. For the first time in Cameroon, atom ratios of $^{236}$U/$^{238}$U were determined, which ranged from $2.31 \times 10^{-8}$ to $4.95 \times 10^{-8}$. Furthermore, secular equilibrium between $^{238}$U and $^{226}$Ra in the sampled soils was studied, activity ratios of $^{226}$Ra/$^{238}$U were out of unity. The $^{137}$ C activity concentrations occur as traces, ranging from below 0.1 to 6.7 Bq kg$^{-1}$.

**Keywords** Secular equilibrium · Atom ratio · Activity ratio · Surface soil · Global fallout · Cameroon

## Introduction

There are several radionuclides present in the environment and are classified into two categories based on their origin, naturally and anthropogenically occurring. The naturally occurring radionuclides can be divided into three different types: the primordial radionuclides that are present in soils and rocks since the formation of the earth such as $^{238}$U-series, $^{232}$Th-series, and $^{40}$K [1]; the radiogenic radionuclides formed from the radioactive decay of $^{238}$U-series and $^{232}$Th-series such as $^{222}$Rn, $^{220}$Rn and their subsequent decay products $^{218}$Po, $^{214}$Pb, $^{214}$Bi, $^{214}$Po, $^{210}$Pb and $^{210}$Po [2]; and the cosmogenic radionuclides such as $^{3}$H, $^{7}$Be, $^{10}$Be, $^{14}$C, $^{26}$Al, $^{32}$Si or $^{36}$Cl produced from the spallation reactions in the upper atmosphere by the interaction of cosmic rays with the atmospheric molecules [3]. On the other hand, the anthropogenically occurring radionuclides also present in the environment are those related to human nuclear activities (atomic bomb testing, nuclear reactor accidents, release from spent nuclear fuel reprocessing facilities, and so on), such as $^{137}$Cs, $^{131}$I, $^{3}$H, $^{90}$Sr or $^{236}$U [4]. Uranium and thorium are present in the soil in the form of different isotopes, and they play an important role in the nuclear industry and present radiological hazards for biological life. Furthermore, after the release from spent nuclear fuel reprocessing facilities, atomic bomb testing and nuclear power plant accidents occurred in the past decades, uranium $^{236}$U and several other anthropogenic radionuclides have been released into the environment [5]. Although Cameroon is a country where nuclear facilities such as power plants or research reactors do not exist, the country uses nuclear technology in various activities, such as in medicine, industry and research. The use of nuclear technology has generated some 200 radioactive sources in use alongside 50 disused sources (those sources considered as nuclear waste, and containing enough radioactive material harmful to humans and the environment). Managing these radioactive sources by keeping them under regulatory control, and assuring the security of the public and environment has been a major focus of the country's National Agency for Radiation Protection (NRPA).

✉ Modibo Oumar Bobbo
bobbomodibo@gmail.com

1 Centre for Nuclear Science and Technology, Institute of Geological and Mining Research, P.O. Box 4110, Yaoundé, Cameroon

2 Nuclear Physics Laboratory, University of Yaoundé I, P.O. Box 810, Yaoundé, Cameroon

3 National Institutes for Quantum Science and Technology, 4-9-1 Anagawa, Inage, Chiba 263-8555, Japan

4 Institute of Radiation Emergency Medicine, Hirosaki University, Aomori 036-8564, Japan

This regulatory body is in charge of both radiation safety and nuclear security [6].

To date, it is a great challenge to measure the anthropogenic sources of uranium isotopes, e.g., $^{236}$U [7–9]. Although there are standard techniques to measure the naturally occurring uranium isotopes such as $^{234}$U, $^{235}$U, $^{238}$U directly by alpha spectrometry or mass spectrometry, most laboratories in developing countries still find it challenging afford [10, 11]. To overcome this handicap, researchers from such laboratories often assumed a radioactive equilibrium between $^{226}$Ra and $^{238}$U. The $^{226}$Ra activity concentration can be accurately determined by gamma-ray spectrometry if the sample is adequately prepared to allow $^{226}$Ra and its decay products $^{214}$Bi and $^{214}$Pb to reach secular equilibrium after 30 days. Thereafter, $^{238}$U activity concentration is deducted from $^{226}$Ra activity concentration by gamma-ray spectrometry. In Cameroon, several research publications dealing with $^{238}$U measurements by gamma-ray spectrometry with the hypothesis of radioactive equilibrium between $^{238}$U and $^{226}$Ra have been reported [12–15]. However, the relationship between $^{238}$U and $^{226}$Ra in these areas should be studied to assess the uncertainties in the measurement of $^{238}$U from $^{226}$Ra.

In the present study, surface soil samples from the seaside, gold mining sites, volcanic terrains, areas of uranium and thorium deposit in Cameroon were collected. The objective was to evaluate their radionuclide contents using two different techniques, i.e. inductively coupled mass spectrometry (ICP-MS) and gamma-ray spectrometry. Meanwhile, the measurement of $^{236}$U to demonstrate its potential sources is new in Cameroon. In addition, the correlation and determination of radioactive or secular equilibrium that exists between $^{238}$U and $^{226}$Ra were done to shed light on the uncertainties of the method used in determining $^{238}$U activity concentration through $^{226}$Ra by gamma-ray spectrometry taking into account the radioactive equilibrium between them from the previous report.

## Materials and methods

### Sampling areas

As shown in Fig. 1, a total of fifteen soil samples were collected in four different regions of Cameroon. Two of them came from the Kitongo area (North Region), a village located in the vicinity of the Kitongo granite burden that hosts a uranium-rich rock [12, 16, 17]. Eight soil samples were collected from the City of Douala which is an industrial and business hub of the Country where previous laboratory and in-situ radioactivity measurements in soil were conducted using the gamma-spectrometry method

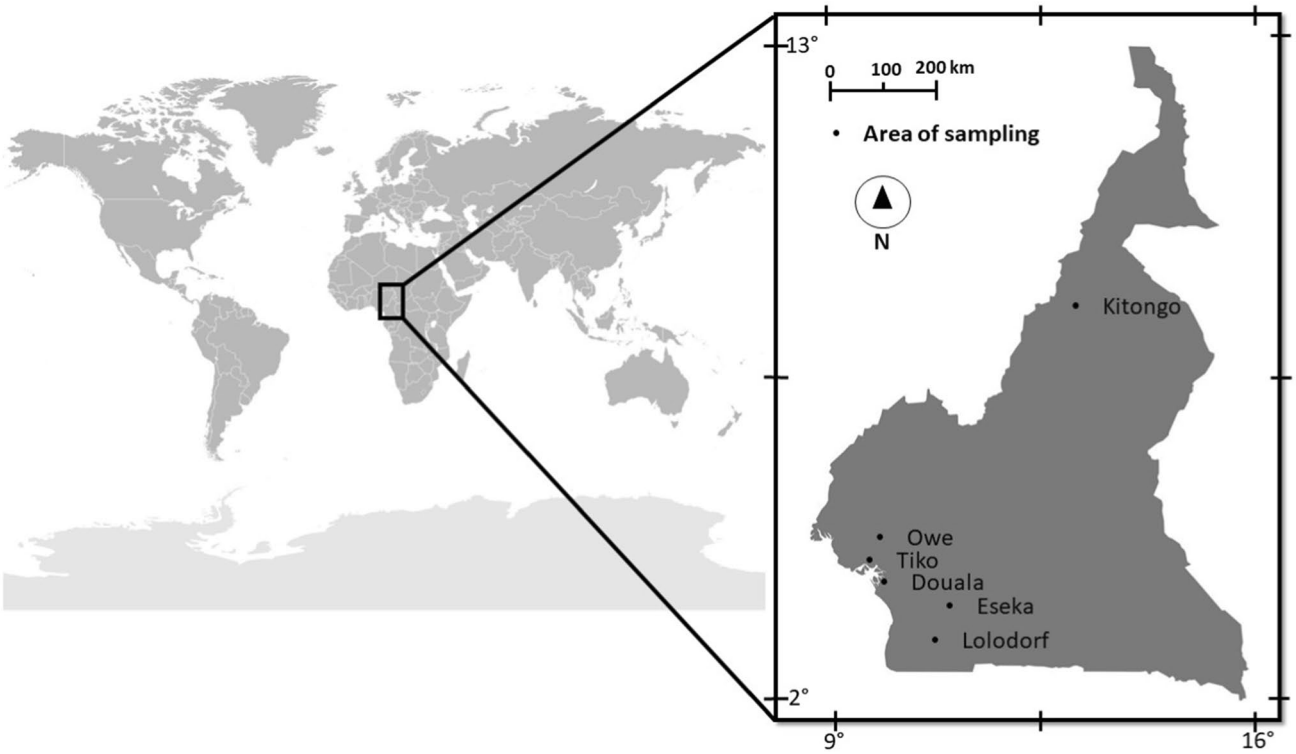


**Fig. 1** Locations of the sampling areas

[18–20]. Three other soil samples were collected from areas of uranium and thorium deposit within Lolodorf and Eseka localities in the southwestern region of the Country. In these localities, abnormally high air dose rates have been reported [21–26]. The two remaining soil samples were each collected from the Tiko and Owe in the South West Region of the country. These two villages are found at the foot of Mount Cameroon, which is an active volcano along the western coast of Africa with the highest peak of 4100 m high [27]. This region has a huge and fertile agricultural land due to its rich volcanic soil.

### Gamma-ray spectrometry analysis

Before the gamma-ray spectrometric analysis, the soil samples were oven-dried at 110 °C for 24 h, then disaggregated and separated using a 2 mm standard stainless sieve. The recovered soil fractions for each sample weighing from 50 to 100 g were placed in the cylindrical plastic container (U-8 type: diameter = 48 mm; high = 58 mm) and sealed tightly using an adhesive glue to avoid the escaping of radon or thoron gases from the sealed containers. The sealed containers were stored for at least 45 days to reach secular equilibrium among $^{226}$Ra, $^{232}$Th, and their respective progeny gamma emitters. Activity concentrations of natural radionuclides were measured using a high purity germanium (HPGe) detector (GEM40190, AMETEK ORTEC, USA) with a relative efficiency of 30% and 1.85 keV energy resolution of Full Width at Half Maximum (FWHM) at 1.33 MeV of $^{60}$Co. The detector was coated inside a 10 cm thick lead shielding, covered with 5 mm of copper and 5 mm of plexiglass layers to ensure a low background configuration. For the gamma-ray spectral data analysis, the detector was coupled with a multi-channel analyzer (MCA-7, Seiko EG&G, Japan), and the computer software gamma vision was used (Seiko EG&G, Japan). Energy and efficiency calibrations of the detector were carried out using the multi-nuclides radioactive standard gamma volume source set that contains $^{109}$Cd, $^{57}$Co, $^{139}$Ce, $^{51}$Cr, $^{85}$Sr, $^{137}$Cs, $^{54}$Mn, $^{88}$Y, and $^{60}$Co radionuclides supplied by the Japan Radioisotope Association with gamma energies ranging from 88 to 1,836 keV and having an overall uncertainty less than 10%. The counting time for every soil sample was set for 260,000 s to lower the counting uncertainty. Assuming secular equilibrium with their progenies in uranium and thorium decay chains, the activity concentrations of $^{226}$Ra and $^{232}$Th were determined. The activity concentration of $^{226}$Ra was determined by weighing the sum of counts in the photoelectric peak channel of the gamma-ray energy line of 609.3 keV from $^{214}$Bi and 352 keV from $^{214}$Pb. To determine $^{232}$Th activity concentration, the counts in the photoelectric peak channel of the single gamma-ray energy line of 911.2 keV from $^{228}$Ac were considered. Activity concentrations of $^{40}$K and $^{137}$Cs were derived directly from the counts in the photoelectric peak channels of the single energy gamma-ray lines 1460.8 and 662 keV, respectively [28, 29].

### Triple-quadrupole inductively coupled plasma-mass spectrometry (ICP-QQQ) MS/MS analysis

Detailed sample digestion and purification were done following procedures described in [16, 30]. 1 g of sieved soil samples were ashed in a muffle furnace at 450 °C for at least 2 h to decompose organic matter. The ashed soil samples were digested with 20 mL concentrated $HNO_3$ for 24 h on a hot plate followed by filtration. After filtration, the eluate was diluted with Milli-Q water to get a 6 M $HNO_3$ solution for DGA resin purification. Following resin preconditioning and sample loading, interference elements were eluted with 20 mL of 6 M $HNO_3$ and 30 mL of 8 M $HNO_3$ solutions. Finally, uranium was eluted with 15 mL of 0.1 M $HNO_3$. Subsequently, the uranium fraction was evaporated to dryness and re-dissolved in 1.5 mL 4% $HNO_3$ The $^{238}$U was measured with an Agilent 8800 ICP-QQQ operated in single MS mode (Agilent Technologies, Santa Clara, CA, USA) after proper dilution of an aliquot of 20 µL sample solution. Uranium atom ratios were obtained using the residual sample solution with the same Agilent 8800 ICP-QQQ operated in tandem MS mode. Under tandem MS (MS/MS) mode measurement conditions, $O_2$ was used as a reaction gas to form $UO^+$ with a flow rate of 0.1 mL min$^{-1}$. The method detection limits for $^{234}$U, $^{235}$U, $^{236}$U and $^{238}$U were $3.04\times10^{-4}$, $2.49\times10^{-6}$, $3.50\times10^{-6}$ and $5.08\times10^{-5}$ Bq kg$^{-1}$, respectively, in 1 g soil sample. The detection limit of $^{236}$U/$^{238}$U atom ratio monitored as $^{236}$U$^{16}$O/$^{238}$U$^{16}$O could reach $10^{-9}$.

## Results and discussion

### Radionuclides content of the soil samples

Eight different radionuclides $^{226}$Ra, $^{232}$Th, $^{40}$K, $^{137}$Cs, $^{234}$U, $^{235}$U, $^{236}$U, and $^{238}$U activities concentration were determined in the soil samples sampled from different areas in Cameroon: Douala, Kitongo, Lolodorf, Eseka, Tiko, and Owe. As shown in Tables 1 and 2, the activity concentrations range from 24.2 to 282.9, 21.6–157.0, 19.7–717.0, < 0.1–6.9, 7.0–269.0, 7.5–420.6, 0.318–18.1, $4.34\times10^{-5}$ – $1.35\times10^{-3}$, and 7.2–266.1 Bq kg$^{-1}$ for $^{226}$Ra, $^{232}$Th, $^{40}$K, $^{137}$Cs, $^{234}$U, $^{235}$U, $^{236}$U, and $^{238}$U, respectively. Meanwhile, other reports from in-situ measurements in the City of Douala show concentrations that vary from 18 to 47 Bq kg$^{-1}$ for $^{238}$U, 21 to 54 Bq kg$^{-1}$ for $^{232}$Th, and 10 to 410 Bq kg$^{-1}$ for $^{40}$K with averages of 29, 38, and 202 Bq kg$^{-1}$, respectively [18]. Accordingly, the concentration obtained

**Table 1** Radionuclides measured by HPGe detector

| Sample ID | $^{232}$Th (Bq kg$^{-1}$) | $^{40}$K (Bq kg$^{-1}$) | $^{226}$Ra (Bq kg$^{-1}$) | $^{137}$Cs (Bq kg$^{-1}$) |
|---|---|---|---|---|
| Kitongo1 | 25.7 ± 1.6 | 717.0 ± 10.5 | 282.9 ± 1.5 | 6.9 ± 0.5 |
| Kitongo2 | 21.6 ± 1.3 | 626.6 ± 9.7 | 96.9 ± 1.0 | 2.2 ± 0.4 |
| Douala1 | 86.3 ± 1.6 | 21.8 ± 4.9 | 29.0 ± 0.6 | < 0.1 |
| Douala2 | 74.4 ± 1.4 | 48.9 ± 4.7 | 27.1 ± 0.6 | < 0.1 |
| Douala3 | 109.1 ± 1.1 | 100.6 ± 3.1 | 45.1 ± 0.4 | < 0.1 |
| Douala4 | 130.3 ± 1.4 | 24.2 ± 3.5 | 50.7 ± 0.5 | < 0.1 |
| Douala5 | 110.2 ± 1.4 | 28.7 ± 3.6 | 42.6 ± 0.5 | < 0.1 |
| Douala6 | 129.7 ± 1.4 | 47.5 ± 3.7 | 46.1 ± 0.5 | < 0.1 |
| Douala7 | 92.2 ± 1.6 | 78.0 ± 5.1 | 38.5 ± 0.6 | < 0.1 |
| Douala8 | 110.8 ± 1.4 | 19.7 ± 3.7 | 36.3 ± 0.5 | < 0.1 |
| Eseka1 | 44.3 ± 1.0 | 95.8 ± 4.0 | 34.1 ± 0.5 | 1.9 ± 0.2 |
| Eseka2 | 157.0 ± 1.7 | 313.9 ± 5.4 | 59.9 ± 0.6 | 2.2 ± 0.2 |
| Lolodorf | 60.1 ± 1.5 | 109.5 ± 6.2 | 24.2 ± 0.7 | < 0.1 |
| Tiko | 33.3 ± 0.8 | 275.9 ± 3.9 | 24.4 ± 0.4 | < 0.1 |
| Owe | 34.1 ± 1.0 | 120.2 ± 4.1 | 37.4 ± 0.5 | 2.7 ± 0.2 |

**Table 2** Radionuclides $^{236}$U and $^{238}$U measured by ICP-MS/MS

| Sample ID | $^{238}$U (Bq kg$^{-1}$) | $^{236}$U (μBq kg$^{-1}$) | Atom ratios $^{236}$U/$^{238}$U |
|---|---|---|---|
| Kitongo1 | 266.1 ± 6.3 | 1340.0 ± 85.6 | (2.64 ± 0.16) × 10$^{-8}$ |
| Kitongo2 | 80.7 ± 2.9 | 403.0 ± 18.4 | (2.61 ± 0.74) × 10$^{-8}$ |
| Douala1 | 10.1 ± 0.2 | 74.3 ± 10.6 | (3.87 ± 0.55) × 10$^{-8}$ |
| Douala2 | 7.2 ± 0.1 | 41.8 ± 8.1 | (3.05 ± 0.59) × 10$^{-8}$ |
| Douala3 | 18.6 ± 0.2 | 175.0 ± 4.1 | (4.95 ± 0.11) × 10$^{-8}$ |
| Douala4 | 22.2 ± 0.3 | 111.0 ± 18.6 | (2.63 ± 0.44) × 10$^{-8}$ |
| Douala5 | 17.5 ± 0.2 | 102.0 ± 10.4 | (3.07 ± 0.31) × 10$^{-8}$ |
| Douala6 | 24.2 ± 0.1 | 107.0 ± 7.0 | (2.32 ± 0.15) × 10$^{-8}$ |
| Douala7 | 17.0 ± 0.3 | 83.2 ± 2.6 | (2.56 ± 0.69) × 10$^{-8}$ |
| Douala8 | 13.4 ± 0.2 | 77.4 ± 3.2 | (3.02 ± 0.12) × 10$^{-8}$ |
| Eseka1 | 12.4 ± 0.1 | 70.4 ± 1.9 | (2.98 ± 0.79) × 10$^{-8}$ |
| Eseka2 | 30.8 ± 0.8 | 146.0 ± 19.0 | (2.478 ± 0.32) × 10$^{-8}$ |
| Lolodorf | 8.6 ± 0.2 | 47.7 ± 4.7 | (2.89 ± 0.27) × 10$^{-8}$ |
| Tiko | 14.1 ± 0.1 | 83.2 ± 5.7 | (3.09 ± 0.21) × 10$^{-8}$ |
| Owe | 30.2 ± 0.3 | 133.0 ± 4.7 | (2.30 ± 0.78) × 10$^{-8}$ |

from laboratory measurements using NaI(Tl) detector varies from 29 to 98 Bq kg$^{-1}$ for $^{238}$U, 29–92 Bq kg$^{-1}$ for $^{232}$Th, and 40–79 Bq kg$^{-1}$ for $^{40}$K, with averages of 60, 57, and 56 Bq kg$^{-1}$, respectively [18]. In comparison, reports on radionuclides measurement in soils within the campuses of the University of Douala show mean values of $^{226}$Ra, $^{232}$Th, and $^{40}$K of 25.5, 66.0, and 39.1 Bq kg$^{-1}$ for Campus 1 and 24.5, 66.7, and 28.2 Bq kg$^{-1}$for Campus 2, respectively [19]. These values are similar to those obtained in the present study for Douala.

In previous studies conducted at another areas, results obtained using the portable NaI(Tl) scintillation detector for in-situ measurement Poli area near Kitongo show activity concentrations for $^{238}$U, $^{232}$Th, and $^{40}$K ranging respectively from 13 to 52, 10–67, and 242–777 Bq kg$^{-1}$ with respective average values of 32, 31, and 510 Bq kg$^{-1}$ [31]. In the Lolodorf area, activity concentrations for $^{226}$Ra, $^{232}$Th, and $^{40}$K from the NaI(Tl) detector ranged from 5 to 120, 2–170, and 50–253 Bq kg$^{-1}$, respectively, with respective averages values of 22, 37, and 98 Bq kg$^{-1}$ [22]. Furthermore, reports on work carried out on soils at Melondo and Gombas localities within the Lolodorf area using CANBERRA alpha spectrometer with ion-implanted silicon detectors show average values of activity concentrations for $^{238}$U, $^{235}$U, $^{234}$U, $^{232}$Th, and $^{226}$Ra of 126 ± 12, 5 ± 1, 131 ± 10, 400 ± 22, and 154 ± 28 Bq kg$^{-1}$, respectively at Melondo; and 170 ± 11, 9 ± 2, 179 ± 12, 200 ± 18, and 416 ± 7 Bq kg$^{-1}$, respectively at Ngombas [23]. Meanwhile, in the same area, the HPGe detector recorded activity concentrations as follow: $^{226}$Ra values vary from 60 to 270 Bq kg$^{-1}$ with a mean value of 130 ± 10 Bq kg$^{-1}$; $^{232}$Th from 100 to 700 Bq kg$^{-1}$ with a mean value of 390 ± 30 Bq kg$^{-1}$; whereas, $^{40}$K vary from 370 to 1,530 Bq kg$^{-1}$ with a mean value of 850 ± 70 Bq kg$^{-1}$ [25]. $^{226}$Ra and $^{232}$Th from the present investigated sites fall within the same range as the values reported in previous studies [12, 18, 19, 31–32]. However, the results for Kitongo and Lolodorf show a contrast between the values of radionuclides measured in soils and rocks [17, 24]. Beyala et al. [24] found activity concentration values from 0.92 to 228 Bq kg$^{-1}$ for $^{235}$U and from 20 to 4868 Bq kg$^{-1}$ for $^{238}$U around Lolodorf, which are higher than those recorded in soils in this study. The present study shows average activity concentration values of $^{226}$Ra (58.0 ± 1.0 Bq kg$^{-1}$) and $^{232}$Th (81 ± 1 Bq kg$^{-1}$) that are above the global averages of 32 and 45 Bq kg$^{-1}$, respectively [1]. Meanwhile,$^{40}$K activity concentration show lower average values of 175 ± 5 Bq kg$^{-1}$ than the global average of 412 Bq kg$^{-1}$ [1]. Generally, previous measurements on $^{40}$K activity concentration appear

higher than the global average [12, 31] but lower in the rainforest and coastal areas [23, 24, 26].

Reports on radioactivity within Cameroon show great variation in different environments within different parts of the country. According to [33], East Cameroon shows average activity concentrations for $^{226}$Ra, $^{232}$Th, and $^{40}$K of 40.1, 29.4, and 216.9 Bq kg$^{-1}$ respectively, while in-situ measurements for $^{40}$K, $^{238}$U and $^{232}$Th gave concentrations of $197 \pm 21$, $37 \pm 13$, and $32 \pm 7$ Bq kg$^{-1}$, respectively [32, 33]. On the other hand, areas of bauxite deposits in the western part of the country gave average values of $671 \pm 272$, $125 \pm 58$, $157 \pm 67$, $6 \pm 3$ and $99 \pm 69$ Bq kg$^{-1}$ for $^{40}$K, $^{226}$Ra, $^{232}$Th, $^{235}$U, and $^{238}$U respectively [34]. Looking at the results, there is an agreement between the measured values and those from previous reports in different areas of the country given that the lowest activity concentrations of $^{40}$K generally fall below the global average in soil samples from the southwestern part of the country (Douala, Eseka, Lolodorf, Tiko, and Owe), and highest in samples from the North (Kitongo).

$^{137}$Cs activity was detected in six samples out of fifteen. The presence of this radionuclide from anthropogenic origin in an environment can be attributed to the global fallout [35]. The $^{137}$Cs values detected in samples from Kitongo, Eseka, and Owe are higher than those reported in previous works in Cameroon [36] but extremely lower than the values measured in regions of eastern and central Europe (close to Chernobyl) and Japan (close to Fukushima), that have suffered severe nuclear power plant accidents [37, 38]. Furthermore, none of the eight samples from Douala gave any detectable $^{137}$Cs activity which could indicate: (1) the deposition of sea salt cations such as $Mg^{2+}$ and $Na^{+}$, replacing Cs ions fixed on soil particle surfaces [38] since Douala is a seaside City, and (2) the significantly high precipitation recorded in the city throughout the year, with the annual average of rainfall of over 3851.2 mm. Reported data (Table 3) in some regions affected by the Chernobyl or Fukushima nuclear power plant accident compared with these results show that $^{137}$Cs activity concentrations in Cameroon soils are extremely low.

Looking at uranium activity concentrations, the results obtained from mass spectrometry measurement on environmental soil in Cameroon serve as baseline data considering that this is the first work done on that aspect in the country. The results for $^{236}$U sources within the surface soils are expressed in atom ratios of $^{236}$U/$^{238}$U (Table 2) show values ranging from $2.31 \times 10^{-8}$ to $4.95 \times 10^{-8}$. These values are within the range of those related to the global fallout summarized by [39]. This suggest that the $^{236}$U contents in environmental soils in Cameroon was caused by the global fallout although other factors may have contributed to these variations.

It is evident that enough interest has not been given to the investigation of the activity of $^{236}$U in surface soils in Africa. Presently, the only $^{236}$U measurement that has been conducted in Southern Africa [40] gave $^{236}$U level of $(0.56 \pm 0.21) \times 10^{6}$ atom/g which corresponds to $(5.24 \pm 1.96) \times 10^{-7}$ Bq kg$^{-1}$ in Maputo (Mozambique) and below detection limit in Durban (South Africa). In Lapalma Spanish Canary Islands on the western coast of Africa, $^{236}$U/$^{238}$U ranged from $10^{-7}$ at the near soil surface to $10^{-9}$ with increasing depth [41].Thus, the $^{236}$U values are higher in Southern Africa (south hemisphere) compared to the ones measured in Cameroon (North hemisphere).

Regarding activity ratios $^{234}$U/$^{238}$U, apart from two samples collected at the Kitongo with values of 1.22 and 1.58, the rest of the samples show $^{234}$U/$^{238}$U activity ratios around 1 (secular equilibrium) i.e., from 0.97 to 1.11 with the average ± SD of $1.02 \pm 0.04$ (Table 4). Based on standards, the activity ratios in undisturbed environments are expected to be equal to 1. Value obtained in all soil samples from test areas have $^{234}$U/$^{238}$U activity ratios within the secular equilibrium range except for two samples with higher values obtained from the Kitongo soil sample. The disequilibrium observed for Kitongo soils could be due to the deposition of dust from the mining activities operating in the area [17].

**Table 3** Atom ratios $^{236}$U/$^{238}$U and $^{137}$Cs activity concentrations determined in different regions near Chernobyl and Fukushima

| Sample's origin | Atom ratios $^{236}$U/$^{238}$U $\times 10^{-8}$ | $^{137}$Cs (Bq kg$^{-1}$) |
|---|---|---|
| Fukushima, Japan (Road dust) [51] | 2.5–26 | – |
| Fukushima, Japan (Soil) [9] | 0.9–13.5 | – |
| Belarus (Chernobyl deposition) [52] | 1548–2661 | – |
| Fukushima, Japan (contaminated soil) [7, 8] | 2.20–19.77 | 4,500,000 |
| Kestanbol, Turkey [53] | – | < 20 |
| Eastern Poland [54] | – | 4.80–40.60 |
| Japan (global fallout) [51] | 1.85–10.90 | – |
| China (background) [30] | 0.63–3.38 | < 5.30 |
| Cameroon, present study | 2.31–4.95 | from < 0.1–6.9 |

**Table 4** Activity concentrations of $^{234}U$, atom and activity ratios $^{234}U/^{238}U$

| Sample ID | $^{234}U$ (Bq kg$^{-1}$) | Atom ratios $^{234}U/^{238}U$ | Activity ratios $^{234}U/^{238}U$ |
|---|---|---|---|
| Kitongo1 | 420.6 ± 10.1 | $8.66\times10^{-5} \pm 9.06\times10^{-7}$ | 1.6 |
| Kitongo2 | 98.5 ± 4.7 | $6.69\times10^{-5} \pm 2.09\times10^{-6}$ | 1.2 |
| Douala1 | 10.4 ± 0.5 | $5.67\times10^{-5} \pm 2.68\times10^{-6}$ | 1.0 |
| Douala2 | 7.5 ± 0.4 | $5.75\times10^{-5} \pm 2.67\times10^{-6}$ | 1.0 |
| Douala3 | 18.3 ± 0.2 | $5.42\times10^{-5} \pm 5.65\times10^{-7}$ | 1.0 |
| Douala4 | 22.5 ± 0.5 | $5.32\times10^{-5} \pm 1.10\times10^{-6}$ | 1.0 |
| Douala5 | 18.0 ± 0.5 | $5.66\times10^{-5} \pm 1.37\times10^{-6}$ | 1.0 |
| Douala6 | 23.7 ± 0.7 | $5.37\times10^{-5} \pm 1.57\times10^{-6}$ | 1.0 |
| Douala7 | 16.5 ± 0.6 | $5.34\times10^{-5} \pm 1.73\times10^{-6}$ | 1.0 |
| Douala8 | 13.7 ± 0.4 | $5.62\times10^{-5} \pm 1.40\times10^{-6}$ | 1.0 |
| Eseka1 | 12.3 ± 0.3 | $5.45\times10^{-5} \pm 1.44\times10^{-6}$ | 1.0 |
| Eseka2 | 29.9 ± 1.9 | $5.32\times10^{-5} \pm 2.96\times10^{-6}$ | 1.0 |
| Lolodorf | 9.7 ± 0.4 | $6.07\times10^{-5} \pm 1.96\times10^{-6}$ | 1.1 |
| Tiko | 14.8 ± 0.6 | $5.74\times10^{-5} \pm 2.15\times10^{-6}$ | 1.0 |
| Owe | 32.3 ± 0.6 | $5.86\times10^{-5} \pm 9.75\times10^{-6}$ | 1.1 |
| Average | | | 1.1 ± 0.2 |

## Variance analysis between $^{238}U$ and $^{226}Ra$ activity concentrations

Activity ratios of $^{226}Ra/^{238}U$ carry out on all soil samples (Table 5) show concentrations ranging from 1.06 to 3.78, with the average ± SD of 2.23 ± 0.74, which indicates radioactive disequilibrium between the two radionuclides. A one-way ANOVA test performed on $^{238}U$ and $^{226}Ra$ activity concentrations show a significant difference between $^{238}U$ activity concentrations and $^{226}Ra$ activity concentrations, with a $p = 0.001$. This suggest that the two radionuclides are not in secular equilibrium in the soil samples in Cameroon and the variations maybe due to the difference in their geochemical properties. Nevertheless, a correlation test between the two radionuclides shows a strong correlation (Fig. 2), with a Pearson correlation coefficient of $r = 0.99$ ($P < 0.01$). A similar strong correlation has also been reported on the studies performed on granitoids samples in Greece [42], and in soil samples from Japan [43–45]. Therefore, a strong correlation coefficient observed and reported between these two radionuclides indicates that the two variables behave similarly in the natural environment (increasing together). Radioactive disequilibrium between $^{238}U$ and $^{226}Ra$ is common in the natural environments. This explains the reason why despite observing a strong correlation in the test samples, the two radionuclides are not in radioactive equilibrium in the soil samples. This might be attributed to the difference in their geochemical properties [46].

**Table 5** Activity concentrations and activity ratios of $^{238}U$ and $^{226}Ra$

| ID | $^{238}U$ (Bq kg$^{-1}$) | $^{226}Ra$ (Bq kg$^{-1}$) | Activity ratios $^{226}Ra/^{238}U$ |
|---|---|---|---|
| Kitongo1 | 266.1 ± 6.3 | 282.9 ± 1.5 | 1.06 |
| Kitongo2 | 80.7 ± 2.9 | 96.9 ± 1.0 | 1.20 |
| Douala1 | 10.1 ± 0.2 | 29.0 ± 0.6 | 2.88 |
| Douala2 | 7.2 ± 0.1 | 27.1 ± 0.6 | 3.78 |
| Douala3 | 18.6 ± 0.2 | 45.1 ± 0.4 | 2.43 |
| Douala4 | 22.2 ± 0.3 | 50.7 ± 0.5 | 2.29 |
| Douala5 | 17.5 ± 0.2 | 42.6 ± 0.5 | 2.44 |
| Douala6 | 24.2 ± 0.1 | 46.1 ± 0.5 | 1.90 |
| Douala7 | 17.0 ± 0.3 | 38.5 ± 0.6 | 2.26 |
| Douala8 | 13.4 ± 0.2 | 36.3 ± 0.5 | 2.71 |
| Eseka1 | 12.4 ± 0.1 | 34.1 ± 0.5 | 2.76 |
| Eseka2 | 30.8 ± 0.8 | 59.9 ± 0.6 | 1.95 |
| Lolodorf | 8.6 ± 0.2 | 24.2 ± 0.7 | 2.81 |
| Tiko | 14.1 ± 0.1 | 24.4 ± 0.4 | 1.73 |
| Owe | 30.2 ± 0.3 | 37.4 ± 0.5 | 1.24 |
| Average ± SD | – | – | 2.23 ± 0.74 |

This disequilibrium has also been reported in most part of the world. For instance, in Egypt, $^{238}U$ and $^{226}Ra$ activity in desert rocks show no equilibrium between the two radionuclides [47], in Greece, the $^{226}Ra/^{238}U$ were closer to unity (unity means that the radionuclides are in radioactive secular equilibrium) in granitic rocks, with several samples showing $^{226}Ra/^{238}U$ out of unity [43]. Elsewhere, the activity ratios $^{226}Ra/^{238}U$ range from 0.64 to 0.72 [48]. Meanwhile in the USA, Rosholt Jr [46] observed radioactive disequilibrium of the uranium series on a total of 138 samples collected in various geological features across the continent [48]. also found out that, 44 samples had an excess uranium vs. radium and 94 had an excess radium vs. uranium form their samples

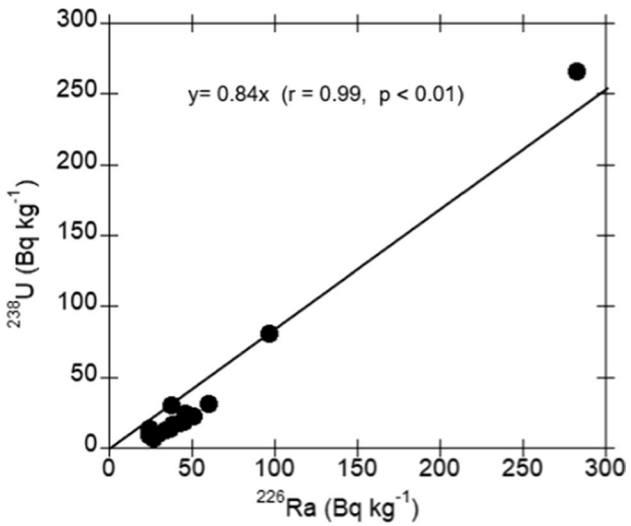


**Fig. 2** Correlation between $^{238}U$ and $^{226}Ra$ activity

population. Based on their interpretation, firstly, the deficiency of daughter product is theoretically uncommon, and can have three explanations, (a) either there is a deposition of uranium with a time less than 300,000 years less than that required time for equilibrium; or (b) there are greater leaching of daughter product than uranium, or (c) there are a combination of uranium deposition and daughter leaching I the environment. Such type of disequilibrium they observed in 44 samples is common with the pitchblende-type ores [46]. Secondly, the disequilibrium characterized with the excess of daughter nuclides found in 94 samples is in general the disequilibrium type found in samples taken from an oxidized environment as a result of leaching of uranium [46]. In our case, the excess of daughter product was found in the fifteen soil samples analyzed. This observation in the Cameroon soils [49] indicates that, samples are collected in oxidized environment and are characterized by a deficiency of uranium which one agree with Rosholt 94 samples taken from oxidized environment [48]. Thus, $^{238}$U in soil cannot be accurately determined by assuming radioactive secular equilibrium with $^{226}$Ra using gamma-ray spectrometry. The calculation of the activity ratios $^{226}$Ra/$^{238}$U appears as a good tool to study the disequilibrium in uranium series and can be applied to detect the discharge of depleted uranium [50]. All the fifteen soil samples of the present study have the activity ratios $^{226}$Ra/$^{238}$U > 1 which characterized a deficiency of $^{238}$U. This could also mean that there is no artificial deposition of $^{238}$U in the sampling areas.

## Conclusion

Several radionuclides activity concentrations and $^{236}$U/$^{238}$U atom ratios were measured in soil samples collected in Cameroon using mass spectrometry and gamma-ray spectrometry. Considering that this was a preliminary study of $^{236}$U in Cameroon soil samples, this can serve as reference in case of future accidental release of nuclear waste fuel in the environment. The results show that the source of $^{236}$U in Cameroon soils are mainly attributable to the global fallout. Low $^{137}$Cs activity concentrations ranging from below 0.1 to 6.9 Bq kg$^{-1}$ were recorded. Meanwhile, the study also shows that $^{238}$U activity concentrations cannot be accurately determined by gamma-ray spectrometry of $^{226}$Ra upon assuming secular equilibrium. All the fifteen soil samples display the activity ratios of $^{226}$Ra/$^{238}$U> 1, indicating a deficiency of $^{238}$U.

**Acknowledgements** To Hirosaki University, Japan for samples analysis. To the Institute of Geological and Mining Research, Cameroon for field work through the Public Investment Budget of the Ministry of Scientific Research and Innovation, Cameroon. To the Terrestrial Radioisotopes in Environment International Conference on Environmental Protection (TRECEIP VIII) where these data have been presented during the Conference and assigned in the book of abstracts of the conference. This work was supported by ERAN Y-23-17.

## Declarations

**Conflict of interest** Author does not have any conflict of interest

## References

1. The United Nation Scientific Committee on the Effect of Atomic Radiation (2008) UNSCEAR 2008 report: sources and effects of ionizing radiation, vol I. United Nations, New York
2. Sýkora I, Holý K, Ješkovský M, Müllerová M, Bulko M, Povinec PP (2017) Long-term variations of radionuclides in the Bratislava air. J Environ Radioact 166:27–35
3. Doering C, Akber R (2008) Beryllium-7 in near-surface air and deposition at Brisbane, Australia. J Environ Radioact 99(3):461–467
4. Yang G, Tazoe H, Yamada M (2016) Determination of $^{236}$U in environmental samples by single extraction chromatography coupled to triple-quadrupole inductively coupled plasma-mass spectrometry. Anal Chim Acta 944:44–50
5. Alvarado JAC, Steinmann P, Estier S, Bochud F, Haldimann M, Froidevaux P (2014) Anthropogenic radionuclides in atmospheric air over Switzerland during the last few decades. Nat Commun 5(1):7
6. IAEA. secure storage, transport and soccer games: improving nuclear security in Cameroon. https://www.iaea.org/newscenter/news/secure-storage-transport-and-soccer-games-improving-nuclear-security-in-cameroon
7. Kasar S, Aono T, Sahoo SK (2021) Precise measurement of $^{234}$U/$^{238}$U, $^{235}$U/$^{238}$U and $^{236}$U/$^{238}$U isotope ratios in Fukushima soils using thermal ionization mass spectrometry. Spectrochim Acta Part B At Spectrosc 180:106161
8. Kasar S, Mishra S, Sahoo SK, Kavasi N, Omori Y, Arae H et al (2021) Sorption-desorption coefficients of uranium in contaminated soils collected around Fukushima Daiichi nuclear power station. J Environ Radioact 233:106617
9. Yang G, Tazoe H, Hayano K, Okayama K, Yamada M (2017) Isotopic compositions of $^{236}$U, $^{239}$Pu, and $^{240}$Pu in soil contaminated by the Fukushima Daiichi nuclear power plant accident. Sci Rep 7(1):13619
10. Hegedűs M, Sas Z, Tóth-Bodrogi E, Szántó T, Somlai J, Kovács T (2016) Radiological characterization of clay mixed red mud in particular as regards its leaching features. J Environ Radioact 162–163:1–7
11. Imani M, Adelikhah M, Shahrokhi A, Azimpour G, Yadollahi A, Kocsis E et al (2021) Natural radioactivity and radiological risks of common building materials used in Semnan Province dwellings Iran. Environ Sci Pollut Res 28(30):41492–41503
12. Oumar Bobbo M, Saïdou NN, Ii JE, Suzuki T, Kudo H, Hosoda M et al (2019) Occupational natural radiation exposure at the uranium deposit of Kitongo, Cameroon. Radioisotopes 68(9):621–630
13. Joel ES, Maxwell O, Adewoyin OO, Olawole OC, Arijaje TE, Embong Z et al (2019) Investigation of natural environmental radioactivity concentration in soil of coastaline area of Ado-Odo/Ota Nigeria and its radiological implications. Sci Rep 12(1):4219
14. Schroeyers W, Sas Z, Bator G, Trevisi R, Nuccetelli C, Leonardi F et al (2018) The NORM4Building database, a tool for radiological assessment when using by-products in building materials. Constr Build Mater 159:755–767

15. Shahrokhi A, Adelikhah M, Chalupnik S, Kovács T (2021) Multivariate statistical approach on distribution of natural and anthropogenic radionuclides and associated radiation indices along the north-western coastline of Aegean Sea, Greece. Mar Pollut Bull 163:112009
16. International Atomic Energy Agency. World Distribution Of Uranium Deposits (UDEPO) IAEA-TECDOC-1843 IAEA TECDOC SERIES. Vienna (2018) ; 106 p
17. Kouske AP, Suh CE, Ghogomu RT, Ngako V (2012) Na-Metasomatism and uranium mineralization during a two-stage albitization at Kitongo, Northern Cameroon: structural and geochemical evidence. Inter J Geosci 03(01):258–279
18. Takoukam Soh SD, Saïdou Hosoda M, Ndjana Nkoulou IIJE, Akata N, Bouba O et al (2018) Natural radioactivity measurements and external dose estimation by car-borne survey in Douala city, Cameroon. Radioprotection 53(4):255–263
19. Ndontchueng MM, Njinga RL, Nguelem EJM, Simo A, Beyala Ateba J (2014) $^{238}$U, $^{235}$U, $^{137}$Cs and $^{133}$Xe in soils from two campuses in University of Douala—Cameroon. Appl Radiat Isot 86:85–89
20. Ndontchueng MM, Mekongtso Nguelem EJ, Simo A, Njinga RL, Joël GSC (2014) Gamma emitting radionuclides in soils from selected areas in Douala–Bassa zone. Littoral Region of Cameroon. ISRN Spectrosc 22(2014):1–8
21. Maurizot P, Abessolo A, Feybesse JL, Johan V PL. Etude et prospection minière du Sud-Ouest Cameroun. Synthèse des travaux du BGRM 1978–1985. Rapport BGRM 85
22. Bineng GS, Saïdou Hosoda M, Tchuente Siaka YF, Naofumi A, Feutseu Talla S, Ele Abiama P, Tokonami S (2020) External Radiation exposure to the public using car-borne survey method in the uranium and thorium bearing Region of Lolodorf Cameroon. Radiat Environ Med 1:13–20
23. Mvondo S, Ben-Bolie GH, Ema'a JME, Ateba PO, Ele abiama P, Ateba JFB (2017) Study of soil-fern transfer of naturally occurring alpha emitting radionuclides in the Southern Region of Cameroon. J Environ Radioact 180:114–119
24. Beyala Ateba JF, Owono Ateba P, Ben-Bolie GH, Ekobena Fouda H, Ele Abiama P, Abega CR et al. (2011) Determination of Uranium in Rocks and Soils of South Cameroon by γ-ray Spectrometry. Radioisotopes: 60(10):399–408.
25. Ele Abiama P, Owono Ateba P, Ben-Bolie GH, Ekobena FHP, el Khoukhi T (2010) High background radiation investigated by gamma spectrometry of the soil in the southwestern region of Cameroon. J Environ Radioact 101(9):739–743
26. Ateba JFB, Ateba PO, Ben-Bolie GH, Abiama PE, Abega CR, Mvondo S (2010) Natural background dose measurements in south Cameroon. Radiat Prot Dosime 140(1):81–88
27. Ngachin M, Garavaglia M, Giovani C, Kwato Njock MG, Nourreddine A (2008) Radioactivity level and soil radon measurement of a volcanic area in Cameroon. J Environ Radioact 99(7):1056–1060
28. IAEA. Handbook of parameter values for the prediction of radionuclide transfer in terrestrial and freshwater environments. International Atomic Energy Agency, Technical Reports Series no. 472.
29. Duong VH, Nguyen TD, Hegedűs M, Tóth-Bodrogi E, Kovács T (2021) Assessment of 232Th, 226Ra, 137Cs, and 40K concentrations and annual effective dose due to the consumption of Vietnamese fresh milk. J Radioanal Nucl Chem 328(3):1399–1404
30. Shao Y, Yang G, Xu D, Yamada M, Tazoe H, Luo M et al (2019) First report on global fallout $^{236}$U and uranium atom ratios in soils from Hunan Province, China. J Environ Radioact 197:1–8
31. Saïdou Shinji T, Hosoda M, Yvette Flore TS, Joseph Emmanuel NN, Naofumi A et al (2019) Natural radiation exposure to the public in the uranium bearing region of Poli, Cameroon: from radioactivity measurements to external and inhalation dose assessment. J Geochem Explor 205:106350
32. Saïdou Tokonami S, Hosoda M, Ndjana Nkoulou IIJE, Akata N, Tchuente Siaka YF (2019) et a Natural radiation exposure to the public in mining and ore bearing regions of Cameroon. Radiat Prot Dosim 184(3–4):391–3966
33. Dallou GB, Ngoa Engola L, Ndjana Nkoulou IIJE, Saïdou, Tcheunte Siaka YF, Bongue D, Kwato Njock MG (2017) NORM measurements and radiological hazard assessment in the gold mining areas of Eastern Cameroon. Radiat Emer Med 6(1):22–28
34. Mekongtso Nguelem EJ, Moyo Ndontchueng M, Motapon O (2016) Determination of 226Ra, 232Th, 40K, 235U and 238U activity concentration and public dose assessment in soil samples from bauxite core deposits in Western Cameroon. Springerplus 5(1253):1–12
35. Fujiwara H (2010) Atmospheric deposition of radioactive cesium($^{137}$Cs)associated with dust events in East Asia. Bull Natl Inst Agro-Environ Sci 85–115.
36. Tchokossa P, Makon TB, Nemba RM (2012) Assessment of radioactivity contents and associated risks in some soil used for agriculture and building materials in Cameroon. J Environ Prot 03(11):1571–1578
37. Hegedűs M, Shiroma Y, Iwaoka K, Hosoda M, Suzuki T, Tamakuma Y (2020) Cesium concentrations in various environmental media at Namie, Fukushima. J Radioanal Nucl Chem 23(1):197–204
38. Gjelsvik R, Steinnes E (2013) Geographical trends in $^{137}$Cs fallout from the chernobyl accident and leaching from natural surface soil in Norway. J Environ Radioact 126:99–103
39. Alam MdF, Hu J, Yang G, Atik Ullah AKM, Khalil MI, Kibria AKMF et al (2021) First study on 236U in environmental samples from Bangladesh by ICP-MS/MS prior to the operation of its first nuclear power plant. J Radioanal Nucl Chem 330(1):103–11
40. Salmani-Ghabeshi S, Chamizo E, Christl M, Miró C, Pinilla-Gil E, Cereceda-Balic F (2018) Presence of $^{236}$U and $^{239,240}$Pu in soils from Southern Hemisphere. J Environ Radioact 192:478–484
41. Srncik M, Steier P, Wallner G (2011) Depth profile of 236U/238U in soil samples in La Palma, Canary Islands. J Environ Radioact 102(6):614–619
42. Papadopoulos A, Christofides G, Koroneos A, Stoulos S, Papastefanou C (2013) Radioactive secular equilibrium in $^{238}$U and $^{232}$Th series in granitoids from Greece. Appl Radiat Isot 75:95–104
43. Hassan NM, Ishikawa T, Hosoda M, Sorimachi A, Tokonami S, Fukushi M et al (2010) Assessment of the natural radioactivity using two techniques for the measurement of radionuclide concentration in building materials used in Japan. J Radioanal Nucl Chem 13(1):15–21
44. Sahoo SK, Hosoda M, Kamagata S, Sorimachi S, Tetsuo I, Tokonami S et al (2011) Thorium, uranium and rare earth elements concentration in weathered Japanese soil samples. Progress in Nuclear Science and Technology 1:416–419
45. Sahoo SK, Hosoda M, Prasad G, Takahashi H, Sorimachi A, Ishikawa T et al (2013) Naturally occurring radionuclides and rare earth elements in weathered Japanese soil samples. Acta Geophysica. https://doi.org/10.2478/s11600-013-0131-3. (**8;61(4):876–85**)
46. Rosholt JJN (1959) Natural radioactive disequilibrium of the uranium series. US Geol Survey Bull 1084-A
47. Abdelmonem AM, Abd El-Samad MA, Hanafi HA et al (2020) Determination of levels of radioactivity of uranium and radium in environmental samples by liquid scintillation counting and alpha spectroscopy. J Nucl Ene Sci Power Generat Technol 9(1):2
48. Ibrahiem NM (2003) Radioactive disequilibrium in the different rock types in Wadi Wizr, the Eastern Desert of Egypt. Appl Radiat Isot 58(3):385–392

49. Yerima BP (2005) In: Publishing T (ed) EVR. Major soil classification systems used in the tropics: soils of Cameroon, vol 1, 1 ed. Victoria BC Canada, Trafford, pp 50–100
50. Besic L, Muhovic I, Asic A, Kurtovic-Kozaric A (2017) Meta-analysis of depleted uranium levels in the balkan region. J Environ Radioact 172:207–217
51. Sakaguchi A, Kawai K, Steier P, Quinto F, Mino K, Tomita J et al (2009) First results on $^{236}$U levels in global fallout. Sci Total Environ 407(14):4238–4242
52. Öztürk BC, Çam NF, Yaprak G (2013) Reference levels of natural radioactivity and $^{137}$Cs in and around the surface soils of Kestanbol pluton in Ezine region of Çanakkale province, Turkey. J Environ Sci Health 15(12):1522–1532
53. Boulyga SF, Becker JS (2001) Determination of uranium isotopic composition and $^{236}$U content of soil samples and hot particles using inductively coupled plasma mass spectrometry. Fresenius J Anal Chem 370(1):612–617
54. Królak E, Karwowska J (2010) Potassium-40 and Cesium-137 in the surface layers of arable soils and food supplies. Polish J of Environ Stud 19(3):599–604